Enhancement of Lithium in Red Clump Stars by the Neutrino Magnetic Moment

Kanji Mori,^{1,2,*} Motohiko Kusakabe,³ A. Baha Balantekin,^{4,2} Toshitaka Kajino,^{2,3,1} and Michael A. Famiano^{5,2}

¹ Graduate School of Science, The University of Tokyo, 7-3-1 Hongo, Bunkyo-ku, Tokyo, 113-0033 Japan
 ² National Astronomical Observatory of Japan, 2-21-1 Osawa, Mitaka, Tokyo 181-8588, Japan
 ³ School of Physics, Beihang University, 37 Xueyuan Road, Haidian-qu, Beijing 100083, China
 ⁴ Department of Physics, University of Wisconsin-Madison, Madison, Wisconsin 53706 USA
 ⁵ Department of Physics, Western Michigan University, Kalamazoo, Michigan 49008 USA

Submitted to ApJL

ABSTRACT

Since ⁷Li is easily destroyed in low temperatures, the surface lithium abundance decreases as stars evolve. This is supported by the lithium depletion observed in the atmosphere of most red giants. However, recent studies show that almost all of red clump stars have high lithium abundances A(Li) > -0.9, which are not predicted by the standard theory of the low-mass stellar evolution. In order to reconcile the discrepancy between the observations and the model, we consider an additional energy loss induced by a neutrino magnetic moment. A(Li) slightly increases near the tip of the red giant branch even in the standard model with thermohaline mixing because of the ⁷Be production by the Cameron-Fowler mechanism, but the resultant ⁷Li abundance is much lower than the observed values. We find that the production of ⁷Be becomes more active if the neutrino magnetic moment is invoked, because themohaline mixing becomes more efficient and a heavier helium core is formed because of the delay of the helium flash. The discrepancy is mitigated when the neutrino magnetic moment of $(2-5) \times 10^{-12} \mu_{\rm B}$ is applied, where $\mu_{\rm B}$ is the Bohr magneton.

Keywords: neutrinos — nuclear reactions, nucleosynthesis, abundances — stars: evolution — stars: low-mass

1. INTRODUCTION

Since 7 Li is a fragile nucleus which is easily destroyed by the proton capture reaction, its surface abundance reflects detailed stellar structure. In low-mass giants, stellar models predict surface lithium depletion (Iben 1967). However, spectroscopic surveys have shown that $\sim 1\%$ of giant stars have the lithium abundance as high as $A(\text{Li}) = \log(\text{Li/H}) + 12 > 1.5$ (e.g. Casey et al. 2016; Yan et al. 2018; Smiljanic et al. 2018; Deepak & Reddy 2019). This is a long-standing problem in our understanding of low-mass stars (Wallerstein & Sneden 1982; Brown et al. 1989).

Corresponding author: Kanji Mori kanji.mori@grad.nao.ac.jp

Stars in the red giant (RG) branch and the red clump (RC) have the similar luminosity and the effective temperature, so the boundary between them is ambiguous in the Hertzsprung-Russell diagram. Some authors have suggested that a part of the lithium-rich giants are RC stars (Silva Aguirre et al. 2014; Monaco et al. 2014). Recent works (Singh, Reddy & Kumar 2019; Singh et al. 2019; Kumar et al. 2020) distinguished RC stars from RGs in data of spectroscopic surveys with the help of asteroseismological data (Bedding et al. 2011; Vrard, Mosser & Samadi 2016). They concluded that all of RC stars have the lithium abundances of A(Li) > -0.9, which are higher than the predicted values by stellar models. This implies that a ubiquitous process produces ⁷Li during or before central helium burning.

The mechanism of this lithium enhancement is under debate. Some authors suggest engulfment of substellar objects which keep high lithium abundances (e.g. Lebzelter et al. 2012; Aguilera-Gómez et al. 2016).

^{*} Research Fellow of Japan Society for the Promotion of Science

Mori et al.

Others discuss in situ production by the Camelon-Fowler (CF) mechanism (Cameron & Fowler 1971). In the hydrogen burning shell, 7 Be is produced via the 3 He(α , γ) 7 Be reaction. The produced 7 Be is conveyed to the stellar surface and decays to 7 Li by the electron capture. In the standard model, the CF mechanism is insufficient to reproduce the abundance in lithium-rich giants. However, Casey et al. (2016) point out that extra mixing induced by the tidal interaction with a binary companion can drive the lithium production.

In order to explain the ubiquitous enhancement of lithium in RC stars, we introduce the additional energy loss induced by the neutrino magnetic moment (NMM), which is denoted as μ_{ν} . The existence of neutrino masses was established by the detection of the neutrino oscillations, starting with atmospheric neutrinos (Fukuda et al. 1998) and later by solar and reactor neutrinos. In the Standard Model of particle physics massive neutrinos have magnetic moments which are too small to be detected by present and near-term future experiments (Shrock 1982; Giunti & Studenikin 2015; Balantekin & Kayser 2018). The current best experimental limit $\mu_{\nu} < 2 \times 10^{-11} \mu_{\rm B}$, where $\mu_{\rm B}$ is the Bohr magneton, comes from the GEMMA experiment (Beda et al. 2013), which measured the scattering cross sections of target electrons and reactor anti-electron neutrinos.

The NMM induces the additional energy loss and affects various stages of stellar evolution for wider mass-range of stars. The effect on the evolution of intermediate-mass stars has recently been studied in detail (Mori et al. 2020) and it was found that in the presence of a sufficiently large NMM the duration of blue giants is shorter and the blue loops are eliminated. Stellar plasma of low-mass stars also is effected by NMM and the helium flash delays (Haft, Raffelt & Weiss 1994). As a result, a heavier inert helium core is formed and the luminosity of the tip of the RG branch (TRGB) increases (e.g. Raffelt 1996). This enables one to use low-mass stars in globular clusters to give a tighter constraint of $\mu_{\nu} < 2.2 \times 10^{-12} \mu_{\rm B}$ (Arceo-Díaz et al. 2015). Also, the delayed helium flash may result in activation of the CF mechanism induced by thermohaline mixing (Sackmann & Boothroyd 1999; Lattanzio et al. 2015).

The aim of this Letter is to show that a sufficiently large NMM can enhance A(Li) in RC stars and reduce the discrepancy between the observations and the theory. Section 2 describes the stellar models and the treatment of the NMM. Section 3 shows the results of our calculations and compares them with the observational data. In Section 4, we summarize our results and discuss the future perspective.

2. METHOD

We use Modules for Experiments in Stellar Astrophysics (MESA; Paxton et al. 2011) version 10398 to construct one-dimensional low-mass stellar models. MESA adopts the equation of state of Rogers & Nayfonov (2002) and Timmes & Swesty (2000) and the opacity of Iglesias & Rogers (1996, 1993) and Ferguson et al. (2005). We adopt nuclear reaction rates compiled by NACRE (Angulo et al. 1999). The adopted nuclear reaction network is pp_extra.net, which includes ^{1,2}H, ^{3,4}He, ⁷Li, ⁷Be, ⁸B, ¹²C, ¹⁴N, ¹⁶O, ²⁰Ne, and ²⁴Mg. Treatment of electron screening is based on Alastuey & Jancovici (1978) and Itoh et al. (1979). The mass loss formula in Reimers (1975) is adopted.

The parameters in our models follow those in Kumar et al. (2020). The initial mass is fixed to $1M_{\odot}$ and the initial metallicity is fixed to be solar: Z=0.0148 (Lodders 2020). However, the initial lithium abundance in the pre-main sequence is set to A(Li)=2.8 to fit data. The mixing length is $\alpha=1.6$ and the thermohaline coefficient is $\alpha_{\text{thm}}=100$ and 50, because A(Li) after the RG branch bump is sensitive to thermohaline mixing.

We consider the plasmon decay and neutrino pair production as the additional energy loss induced by the NMM. The energy loss rate due to the plasmon decay is given by (Haft, Raffelt & Weiss 1994; Heger et al. 2009)

$$\epsilon_{\rm plas}^{\mu} = 0.318 \left(\frac{\omega_{\rm pl}}{10 \text{ keV}}\right)^{-2} \left(\frac{\mu_{\nu}}{10^{-12} \mu_{\rm B}}\right)^{2} \epsilon_{\rm plas}, \quad (1)$$

where $\epsilon_{\rm plas}$ is the standard plasmon decay rate (Itoh et al. 1996) and $\omega_{\rm pl}$ is the plasma frequency (Raffelt 1996)

$$\omega_{\rm pl} = 28.7 \text{ eV} \frac{(Y_{\rm e}\rho)^{\frac{1}{2}}}{(1 + (1.019 \times 10^{-6} Y_{\rm e}\rho)^{\frac{2}{3}})^{\frac{1}{4}}},$$
 (2)

where $Y_{\rm e}$ is the electron mole fraction and ρ is the density in units of g cm⁻³. The energy loss rate due to the pair production is given by (Heger et al. 2009)

$$\epsilon_{\text{pair}}^{\mu} = 1.6 \times 10^{11} \text{ erg g}^{-1} \text{ s}^{-1} \left(\frac{\mu_{\nu}}{10^{-10} \mu_{\text{B}}}\right)^{2} \frac{e^{-\frac{118.5}{T_{8}}}}{\rho_{4}},$$
(3)

where T_8 is the temperature in units of 0.1 GK and $\rho_4 = \rho/(10^4 \text{ g cm}^{-3})$.

Fig. 1 shows the energy loss rates with $\mu_{\nu} = 5 \times 10^{-12} \mu_{\rm B}$ at $\rho = 10^6$ g cm⁻³, which is the typical central density at the helium flash. At the temperature of $\sim 10^8$ K, the enhanced energy loss rate is comparable with the standard rate. Also, it is seen that the pair production is negligible in the temperature range of interest.

3. RESULT

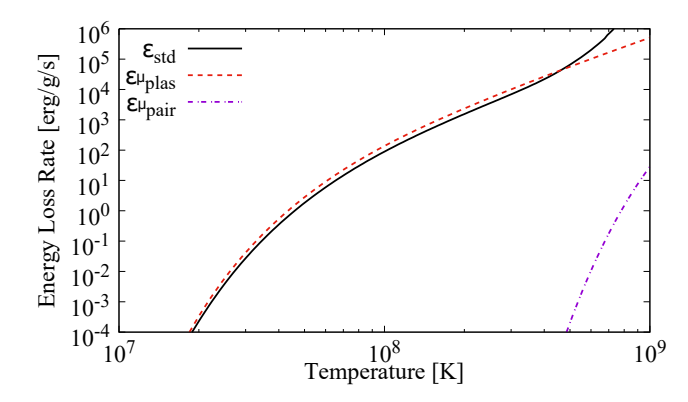


Figure 1. The energy loss rates induced by the neutrino emission with $\mu_{\nu} = 5 \times 10^{-12} \mu_{\rm B}$. The density of $\rho = 10^6$ g cm⁻³ is assumed. The black line shows the total standard rate and the other lines show the rates enhanced by the NMM.

$\alpha_{ m thm}$	μ_{12}	$M_{ m He,TRGB}/M_{\odot}$	$\log(L/L_{\odot})_{\mathrm{TRGB}}$	$A(\mathrm{Li})_{\mathrm{RC}}$
100	0	0.467	3.39	-0.90
100	2	0.480	3.46	-0.57
100	3	0.490	3.52	-0.23
100	4	0.500	3.57	0.10
100	5	0.509	3.61	0.38
50	0	0.467	3.39	-0.56
50	2	0.480	3.46	-0.39
50	3	0.490	3.52	-0.16
50	4	0.500	3.56	0.12
50	5	0.509	3.60	0.39

Table 1. The parameters of the models. The zero age main sequence mass and the initial metallicity are fixed to $M_{\rm ZAMS}=1M_{\odot}$ and Z=0.0148, respectively. $\alpha_{\rm thm}$ is the thermohaline coefficient, μ_{12} is the NMM, $M_{\rm He,TRGB}$ is the mass of the helium core at the TRGB, $L_{\rm TRGB}$ is the luminosity at the TRGB, and $A({\rm Li})_{\rm RC}$ is the lithium abundance of RC stars. Since $A({\rm Li})$ decreases during the evolution of RC stars, the initial values just after the helium flash are shown.

We perform stellar evolution calculations with $\mu_{12} = 2 - 5$, where $\mu_{12} = \mu_{\nu}/(10^{-12}\mu_{\rm B})$. The adopted parameters and results are summarized in Table 1.

Fig. 2 shows the evolution of the stellar models in the L-A(Li) plane, where L is the luminosity. The upper panel adopts $\alpha_{\text{thm}} = 100$ and the lower panel adopts $\alpha_{\text{thm}} = 50$. The evolution starts from a low luminosity (the lower-left side of Fig. 2). The lithium abundance A(Li) stays constant during the main sequence. When the star reaches the main-sequence turnoff at $\log(L/L_{\odot}) = 0.4$, A(Li) starts to decrease from 2.4 to 0.8. This is because surface lithium is conveyed to the stellar interior due to the first dredge-up (Iben 1967),

and is destroyed by the proton capture. The lithium depletion becomes slower as the star evolves, but A(Li)starts to decrease again when the star reaches the RG branch bump at $\log(L/L_{\odot}) = 1.5$. At this point, the star develops thermohaline mixing between the convective envelope and the hydrogen burning shell (Charbonnel & Zahn 2007; Lattanzio et al. 2015). This happens because the mean molecular weight is inverted by ³He(³He, $(2p)^4$ He. Because of thermohaline mixing, lithium in the envelope is conveyed to the inner hot region and destroyed. One can see that A(Li) after the RG branch bump is smaller when a larger $\alpha_{\rm thm}$ is adopted. The decrease of A(Li) stops when $\log(L/L_{\odot}) = 3.2$ and it starts increasing. This is because thermohaline mixing becomes more effective as the star expands (Lattanzio et al. 2015). The effective mixing helps the CF mechanism work and hence increases A(Li). After the TRGB, the core becomes non-degenerate because of the helium flash and L decreases suddenly. As a result, core helium burning begins and a RC star is formed.

 $A({\rm Li})$ and L at the TRGB increase when a larger value of μ_{ν} is adopted. The fact that TRGB stars become luminous when μ_{ν} is adopted has been used to constrain μ_{ν} (e.g. Raffelt 1996; Arceo-Díaz et al. 2015). Fig. 3 shows the evolution of $A({\rm Li})$ as a function of the helium core mass $M_{\rm He}$ when $\alpha_{\rm thm}=100$. The peaks around $M_{\rm He}\sim 0.5 M_{\odot}$ correspond to the helium flash. One can confirm that $A({\rm Li})$ at the TRGB is higher when μ_{ν} is larger.

The physical mechanisms of the lithium enhancement are twofold. Central helium burning is ignited when the nuclear energy production exceeds the energy loss rate. When $\mu_{\nu} > 0$ is adopted, the helium flash is delayed by the additional energy loss and hence the helium core at the ignition of central helium burning becomes heavier. Therefore the CF mechanism can continue to produce more ⁷Li and A(Li) in RC stars becomes higher.

It is seen from Fig. 3 that A(Li) starts to deviate from the standard model even before the helium flash. This is explained by changes of stellar structure induced by the NMM. Fig. 4 shows the thermohaline diffusion coefficient D_{thm} and the mass fractions of ⁷Li and ⁷Be for the models with $\mu_{12}=0$, 2, and 5 in the region where thermohaline mixing is effective. In this figure, the helium core mass is fixed to $M_{\text{He}}=0.45M_{\odot}$. When a larger NMM is adopted, the radius of the helium core becomes smaller and the density in the envelope decreases. The smaller density results in a larger thermal diffusivity and a larger D_{thm} (Lattanzio et al. 2015). Since ⁷Be produced via ³He(α , γ) is conveyed to the outer region by thermohaline mixing, the more efficient mixing leads to a larger A(Li).

4 Mori et al.

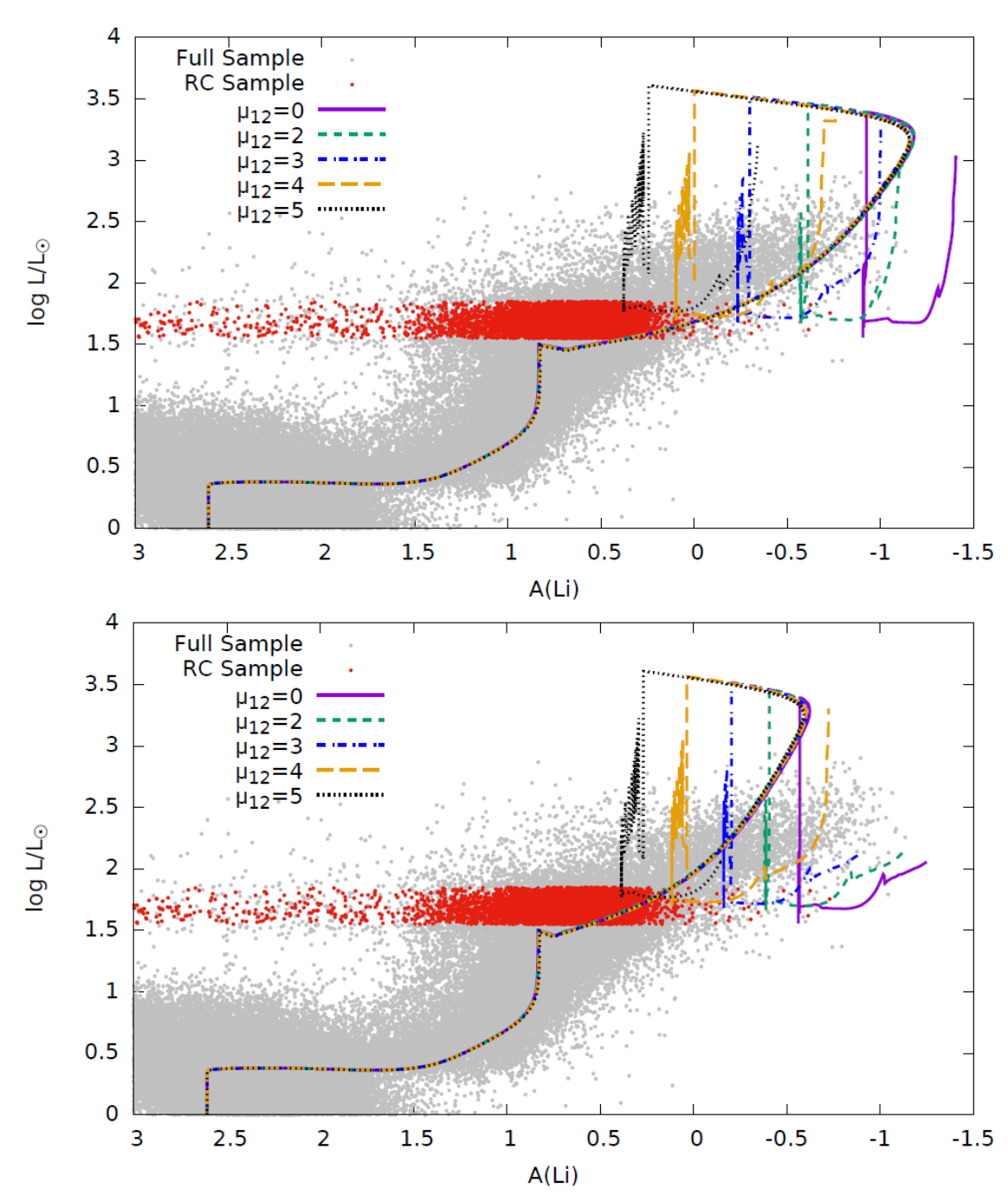


Figure 2. The lines show the evolution of our models with $\mu_{12} = 0 - 5$ in the L - A(Li) plane. The upper panel adopts $\alpha_{\text{thm}} = 100$ and the lower panel adopts $\alpha_{\text{thm}} = 50$. The grey dots are GALAH DR2 samples (Buder et al. 2018) with reliable lithium abundances and the red dots are RC samples selected by Kumar et al. (2020).

Recently, the GALAH (Galactic Archaeology with HERMES) survey second data release (DR2) provided spectroscopic data of 342,682 stars in the Milky Way (Buder et al. 2018). Kumar et al. (2020) selected stars with $\log L/L_{\odot} \in [1.55,~1.85]$ and the effective temperature $T_{\rm eff} \in [4650,~4900]$ K from the GALAH DR2 samples and identified them as RC stars. Kumar et al. (2020) used GALAH samples that overlap with an

astroseismic catalog (Ting, Hawkins & Rix 2018) to distinguish RC and RG stars. They concluded that the contamination of RGs in their RC samples accounts for only $\sim 10\%$.

Kumar et al. (2020) found that the lithium abundance in RC stars is distributed around $A(\text{Li}) \sim 0.71 \pm 0.39$. This ubiquitous enhancement of lithium has not been predicted by stellar models. When the NMM is not

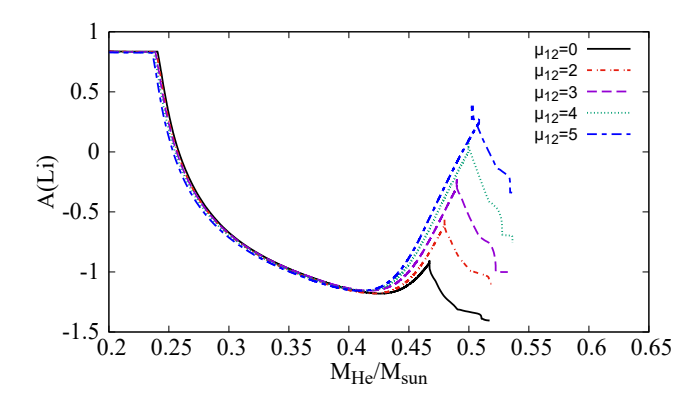
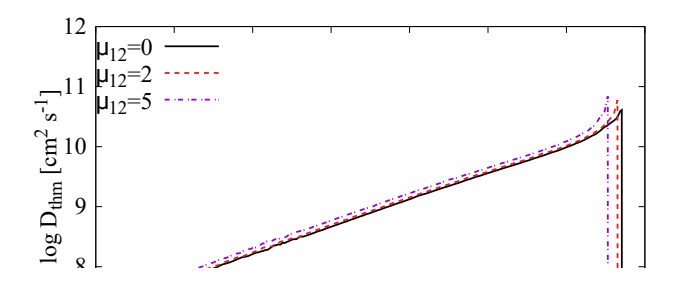


Figure 3. The evolution of the surface lithium abundance as a function of the helium core mass. The thermohaline coefficient is fixed to $\alpha_{\rm thm}=100$.



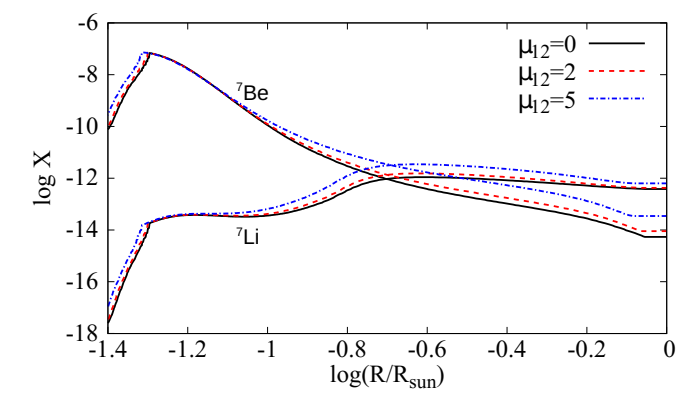


Figure 4. Structure of our model when $\mu_{12}=0$, 2, and 5 and $M_{\rm He}=0.45M_{\odot}$. The upper panel shows the thermohaline diffusion coefficient and the lower panel shows the mass fractions of ⁷Li and ⁷Be as a function of the radius. The thermohaline coefficient is fixed to $\alpha_{\rm thm}=100$.

adopted in our model, the lithium abundance in RC stars is only $A(\text{Li}) = -0.90 \ (-0.56)$ when $\alpha_{\text{thm}} = 100 \ (50)$. We find that, if $\mu_{12} = 5$ is adopted, A(Li) reaches 0.38 (0.39), which is consistent with the observed A(Li). When α_{thm} is larger, ⁷Li is destroyed to a greater extent after the RG branch bump and thus A(Li) in RC stars becomes smaller. Although A(Li) is not sufficiently

large when $\mu_{12} = 2-4$ in both cases, the discrepancy in A(Li) becomes smaller if the NMM is adopted. The additional energy loss induced by the NMM is thus a candidate of a ubiquitous mechanism of the high A(Li) in RC stars.

Traditionally, giants with A(Li) > 1.5 have been called lithium-rich giants (Brown et al. 1989). It is difficult to explain such extremely high lithium abundances with the NMM only. Kumar et al. (2020) point out that lithium-rich giants with A(Li) > 1.5 account only for $\sim 3.0\%$ of RC stars. The rare population implies another mechanism which works only in a certain kind of stars.

4. DISCUSSION

In this Letter, we discussed the effects of the NMM on A(Li) in RC stars. We found that the production of ⁷Li near the TRGB is activated when $\mu_{12}=2-5$ is adopted. The ubiquitous high A(Li) in RC stars (Kumar et al. 2020) may be explained by the additional energy loss induced by the NMM. This value of the neutrino magnetic moment is smaller than current limits obtained from the reactor experiments, but is very close to the constraint obtained from low-mass stars in globular clusters.

The destruction and production of ^7Li are dependent on deep mixing including thermohaline mixing (Charbonnel & Zahn 2007; Lattanzio et al. 2015) and magnetic buoyancy (Busso et al. 2007). It is desirable to investigate these mechanisms in detail. Also, the additional energy loss can be induced by other physics like extra dimensions (Cassisi et al. 2000) and axion-like particles (Raffelt & Dearborn 1987; Ayala et al. 2014). Since they are expected to result in the similar enhancement of A(Li), they can be a candidate of the mechanism of the lithium enhancement as well.

The enhancement of energy loss rate from neutrino emission affects Li abundances on stellar surfaces through a change in stellar structure, including He core mass and total mass, and its evolution time scale. This characterizes the current theoretical prediction distinguished from other possibilities. For example, in addition to the ⁷Be production via the ³He(α,γ) reaction operating deep inside the stars, stellar surfaces can be polluted from outside by accretion of companion stellar ejecta or nucleosynthesis via flare-accelerated nuclei on stellar surfaces. If the observed high abundances of Li originate from nucleosynthesis in companion asymptotic giant branch stars (Ventura & D'Antona 2010), observed stars can have enhanced abundances of carbon and s-nuclei. On the other hand, if nuclear reactions of flare-accelerated nuclei (Tatischeff & Thibaud 2007) are providing ^{6,7}Li, the isotopic fraction of ⁶Li is expected

6 Mori et al.

to be high. Furthermore, the observed Li-rich stars must be associated with very strong flare activities and simultaneous production of Be and B. In this way, respective possibilities are associated with different astronomical observables to be measured in future.

ACKNOWLEDGMENTS

We thank Yerra Bharat Kumar and Gang Zhao for providing observational data. K.M. is supported by JSPS KAKENHI Grant Number JP19J12892. T.K. is supported in part by Grants-in-Aid for Scientific Research of JSPS (17K05459, 20K03958). A.B.B. is supported in part by the U.S. National Science Foundation Grants No. PHY-1806368 and PHYS-2020275. M.A.F. is supported by National Science Foundation Grant No. PHY-1712832 and by NASA Grant No. 80NSSC20K0498. M.A.F. and A.B.B. acknowledge support from the NAOJ Visiting Professor program.

Software: MESA (Paxton et al. 2011)

REFERENCES

- Aguilera-Gómez, C., Chanamé, J., Pinsonneault, M. H., et al. 2016, ApJL, 833, L24
- Alastuey, A., & Jancovici, B. 1978, ApJ, 226, 1034
- Angulo, C., Arnould, M., Rayet, M., et al. 1999, NuPhA, $656,\,3$
- Arceo-Díaz, S., Schröder, K.-P., Zuber, K., et al. 2015, Astroparticle Physics, 70, 1
- Ayala, A., Domínguez, I., Giannotti, M., et al. 2014, PhRvL, 113, 191302
- Balantekin, A. B., & Kayser, B. 2018, Annual Review of Nuclear and Particle Science, 68, 313
- Beda, A. G., Brudanin, V. B., Egorov, V. G., et al. 2013, Physics of Particles and Nuclei Letters, 10, 139
- Bedding, T. R., Mosser, B., Huber, D., et al. 2011, Nature, 471, 608
- Brown, J. A., Sneden, C., Lambert, D. L., et al. 1989, ApJS, 71, 293
- Buder, S., Asplund, M., Duong, L., et al. 2018, MNRAS, 478, 4513
- Busso, M., Wasserburg, G. J., Nollett, K. M., et al. 2007, ApJ, 671, 802
- Cameron, A. G. W. & Fowler, W. A. 1971, ApJ, 164, 111
- Casey, A. R., Ruchti, G., Masseron, T., et al. 2016, MNRAS, 461, 3336
- Cassisi, S., Castellani, V., Degl'Innocenti, S., et al. 2000, Physics Letters B, 481, 323
- Charbonnel, C. & Zahn, J.-P. 2007, A&A, 467, L15
- Deepak & Reddy, B. E. 2019, MNRAS, 484, 2000
- Ferguson, J. W., Alexander, D. R., Allard, F., Barman, T., Bodnarik, J. G.,
- Fukuda, Y., Hayakawa, T., Ichihara, E., et al. 1998, PhRvL, 81, 1562
- Giunti, C., & Studenikin, A. 2015, Reviews of Modern Physics, 87, 531
- Haft, M., Raffelt, G., & Weiss, A. 1994, ApJ, 425, 222

- Heger, A., Friedland, A., Giannotti, M., et al. 2009, ApJ, 696, 608
- Iben, I. 1967, ApJ, 147, 624
- Iglesias, C. A., & Rogers, F. J. 1993, ApJ, 412, 752
- Iglesias, C. A., & Rogers, F. J. 1996, ApJ, 464, 943
- Itoh, N., Totsuji, H., Ichimaru, S., & Dewitt, H. E. 1979, ApJ, 234, 1079
- Itoh, N., Hayashi, H., Nishikawa, A., et al. 1996, ApJS, 102, 411
- Kumar, Y. B., Reddy, B. E., Campbell, S. W., et al. 2020, Nature Astronomy, doi:10.1038/s41550-020-1139-7
- Lattanzio, J. C., Siess, L., Church, R. P., et al. 2015, MNRAS, 446, 2673
- Lebzelter, T., Uttenthaler, S., Busso, M., et al. 2012, A&A, 538, A36
- Lodders, K. 2020, Solar Elemental Abundances, in The Oxford Research Encyclopedia of Planetary Science, Oxford University Press
- Monaco, L., Boffin, H. M. J., Bonifacio, P., et al. 2014, A&A, 564, L6
- Mori, K., Balantekin, A. B., Kajino, T., et al. 2020, arXiv:2008.08393
- Paxton, B., Bildsten, L., Dotter, A., et al. 2011, ApJS, 192, 3
- Raffelt, G. G. 1996, Stars as laboratories for fundamental physics: the astrophysics of neutrinos (Chicago: The University of Chicago Press)
- Raffelt, G. G. & Dearborn, D. S. P. 1987, PhRvD, 36, 2211Reimers, D. 1975, Memoires of the Societe Royale desSciences de Liege, 8, 369
- Rogers, F. J., & Nayfonov, A. 2002, ApJ, 576, 1064
- Sackmann, I.-J. & Boothroyd, A. I. 1999, ApJ, 510, 217
- Shrock, R. E. 1982, Nuclear Physics B, 206, 359
- Silva Aguirre, V., Ruchti, G. R., Hekker, S., et al. 2014, ApJL, 784, L16

Singh, R., Reddy, B. E., & Kumar, Y. B. 2019, MNRAS, 482, 3822

Singh, R., Reddy, B. E., Bharat Kumar, Y., et al. 2019, ApJL, 878, L21

Smiljanic, R., Franciosini, E., Bragaglia, A., et al. 2018, A&A, 617, A4

Tatischeff, V. & Thibaud, J.-P. 2007, A&A, 469, 265

Timmes, F. X., & Swesty, F. D. 2000, ApJS, 126, 501Ting, Y.-S., Hawkins, K., & Rix, H.-W. 2018, ApJL, 858,L7

Yan, H.-L., Shi, J.-R., Zhou, Y.-T., et al. 2018, Nature Astronomy, 2, 790

Ventura, P., & D'Antona, F. 2010, MNRAS, 402, L72
Vrard, M., Mosser, B., & Samadi, R. 2016, A&A, 588, A87
Wallerstein, G. & Sneden, C. 1982, ApJ, 255, 577